High-Contrast Interference of Ultracold Fermions

Philipp M. Preiss,[1,*] Jan Hendrik Becher,[1] Ralf Klemt,[1] Vincent Klinkhamer,[1]
Andrea Bergschneider,[1,†] Nicolò Defenu,[1,2] and Selim Jochim[1]
[1]*Physics Institute, Heidelberg University, 69120 Heidelberg, Germany*
[2]*Institute for Theoretical Physics, Heidelberg University, 69120 Heidelberg, Germany*

(Received 30 November 2018; published 12 April 2019)

Many-body interference between indistinguishable particles can give rise to strong correlations rooted in quantum statistics. We study such Hanbury Brown–Twiss-type correlations for number states of ultracold massive fermions. Using deterministically prepared ^{6}Li atoms in optical tweezers, we measure momentum correlations using a single-atom sensitive time-of-flight imaging scheme. The experiment combines on-demand state preparation of highly indistinguishable particles with high-fidelity detection, giving access to two- and three-body correlations in fields of fixed fermionic particle number. We find that pairs of atoms interfere with a contrast close to 80%. We show that second-order density correlations arise from contributions from all two-particle pairs and detect intrinsic third-order correlations.

DOI: 10.1103/PhysRevLett.122.143602

Many-body interference describes processes by which noninteracting particles acquire strong correlations solely due to their quantum statistics [1]. In such cases, interference occurs between many-particle paths and the enhancement or suppression of particular outcomes is dictated by the exchange statistics of the particles.

The most famous example of many-body interference is the "bosonic bunching" of photons, as observed by Hanbury Brown and Twiss in the development of stellar intensity interferometry [2,3]. The experimental [4,5] and theoretical [6] study of correlations in photon fields has been driving the development of quantum optics [7].

In contrast to the statistical behavior of bosons, which can in certain cases be described in terms of classical waves [2], the interference of fermionic particles is a uniquely quantum mechanical phenomenon. Experimental access to correlations arising from fermionic interference allows the study of quantum systems through intensity interferometry, for example, in heavy ion collisions [8] and ultracold atom systems [9]. Fermionic interference and associated anticorrelations have been observed for thermal sources of neutrons [10] and cold atoms [11], as well as electrons in free space [12] and in solid state [13,14]. Interference between fermionic number states, however, has been far more elusive: Few particle species amenable to single-particle control possess fermionic statistics, and realizing high-quality single-fermion sources is an outstanding experimental challenge. Recent advances in this direction have enabled the observation of two-fermion interference in semiconductor architectures [15] and double ionization processes [16].

Here, we observe high-contrast interference of fermionic particles in pure quantum states of ultracold atoms. We use optical tweezers as a configurable, deterministic source of noninteracting fermions [17,18]. The particles interfere

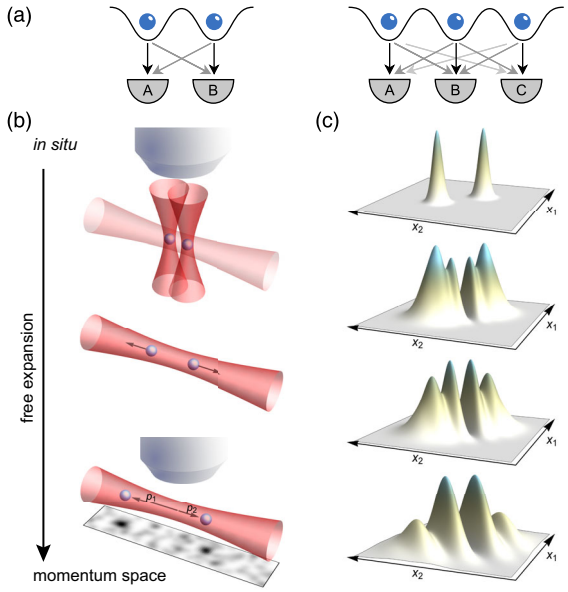

FIG. 1. Many-body interference of fermionic particles. (a) The coincidence events for two detectors monitoring single-particle sources are given by the available sets of many-body paths. For indistinguishable particles, the paths add coherently where the sign of their interference depends on quantum statistics. Two sources emitting indistinguishable fermions display suppressed coincidence counts. In a setting with more particles, correlations between detectors arise due to interference of all many-body paths. (b) We realize the thought experiment from Fig. 1(a) using ultracold fermions in optical tweezers. Time-of-flight expansion is performed in an optical dipole trap aligned with the x axis connecting the tweezers, and particles are detected in free-space fluorescence imaging. (c) The probability distribution $|\Psi(x_1, x_2)|^2$ (plotted for the two-mode case) evolves from localized to delocalized states during time of flight but retains a node at $x_1 = x_2$ due to fermionic antisymmetry.

during a ballistic time of flight and are detected with high fidelity. We observe periodic antibunching of two fermions with close to full contrast. Adding a third source to the system, we measure the second- and third-order correlation properties of a three-fermion field and determine the contribution of intrinsic third-order correlations [19,20].

Our experiments use ^{6}Li atoms in the same internal state initialized in optical microtraps separated by tunable distances of several microns (see Fig. 1) [21]. Within the regime of s-wave interactions, fermions in the same internal state do not interact, and the particles behave as ideal free fermions. We release the atoms simultaneously into a weak, elongated optical dipole trap aligned with the axis connecting the tweezers. The dipole trap enables a one-dimensional time-of-flight measurement, wherein the wave packets remain localized in the transverse directions. In the weakly confined x direction, evolution in the approximately harmonic confining potential linearly maps initial momenta onto the final position [22], similar to free-space time-of-flight schemes [9,23]. The single-particle wave functions are initially localized to ∼250 nm and expand to a size of ∼400 μm before detection. We extract the position of individual atoms along the axis of the dipole trap with a free-space state-resolved imaging technique [24] [see Fig. 1(b)]. Any correlations can be interpreted as position correlations upon interference, or equivalently as momentum correlations in the initial state.

In a first set of experiments, we study the interference of fermionic particles from two tweezers separated by a distance of $a = 1.7$ μm. The tweezers are loaded independently from a degenerate Fermi gas and initialized with the $n = 1$ number state with a probability of 97(2)% per tweezer. Residual tunnel couplings of, at most, 0.1 Hz are negligible on the ∼100 ms timescale of the experiment. This configuration corresponds to the scenario sketched in Figs. 1(a) and 1(c): Fermionic correlations arise due to destructive interference of two sets of two-particle paths, or equivalently from the preservation of antisymmetry of the two-particle wave function during time of flight. This experiment directly realizes the fermionic analog of the Ghosh-Mandel experiment [4].

Our method extends the noise-correlation analysis, which was pioneered on many-body lattice systems [9,23,25,26], to measurements of full atomic correlations of a single, nearly pure quantum state. The availability of individual particle momenta allows us to obtain normal-ordered correlation functions that are free from autocorrelation peaks at a zero interparticle distance [21,27]. We record the momenta of the particles for each experimental run and construct the momentum density $\langle n_k \rangle$ at wave vector k and its second-order correlator $\langle :\hat{n}_{k1}\hat{n}_{k2}: \rangle$ from several thousand realizations ($\langle : \cdot \cdot : \rangle$ denotes normal ordering). We only retain data from runs where two particles were successfully prepared and detected, which correspond to about 80% of the data.

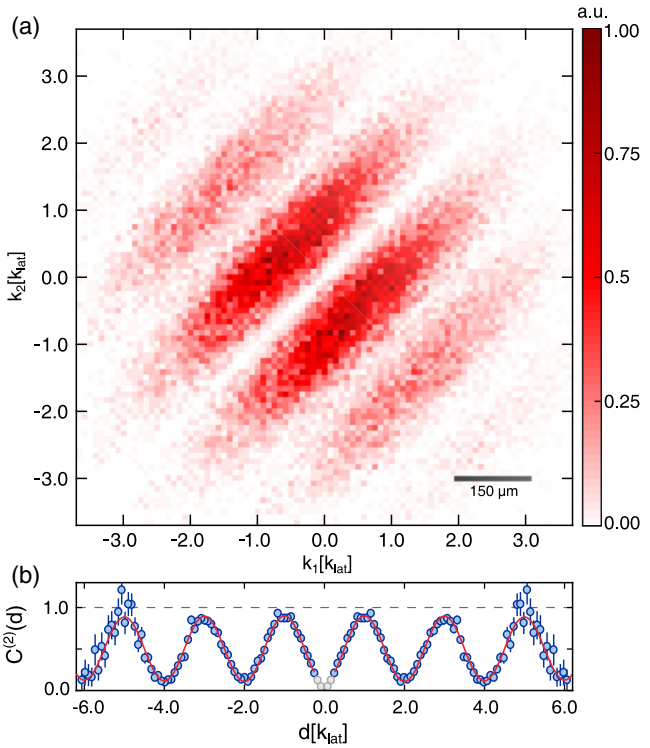

FIG. 2. Interference of two fermions. (a) Measured momentum correlator $\langle :\hat{n}_{k1}\hat{n}_{k2}: \rangle$ for two particles prepared in two optical tweezers, showing strong fermionic antibunching. The data are symmetric about the diagonal $k_1 = k_2$ by construction, but we plot the full correlator for visual clarity. (b) The normalized correlator $C^{(2)}(d)$ shows a clear, almost full sinusoidal modulation in the relative momentum d. We extract a contrast of 79(2)% by fitting a cosine to the data, excluding the grayed out points near the origin, for which coincidences cannot reliably be detected.

In Fig. 2(a), the experimentally measured momentum correlator is shown. The strong correlations in the relative momentum $d = k_1 - k_2$ immediately demonstrate the nonseparability of the correlator into single-particle momenta. The modulations occur on a "lattice" momentum scale $k_{\mathrm{lat}} = \pi/a$ and carry an envelope set by the single-particle on-site momentum distribution.

As correlations do not depend on the center of mass momentum, we define a normalized correlation function [9,23]

$$C^{(2)}(d) = \frac{\int \langle :\hat{n}_k \hat{n}_{k+d}: \rangle dk}{\int \langle \hat{n}_k \rangle \langle \hat{n}_{k+d} \rangle dk}. \tag{1}$$

The correlation function in Fig. 2(b) exhibits close to full-contrast sinusoidal oscillations consistent with a minimum at $d = 0$, corresponding to strong fermionic antibunching. The grayed out points near $d = 0$ mark the region of particle separation below 30 μm, where two particles cannot be distinguished reliably and coincidences cannot

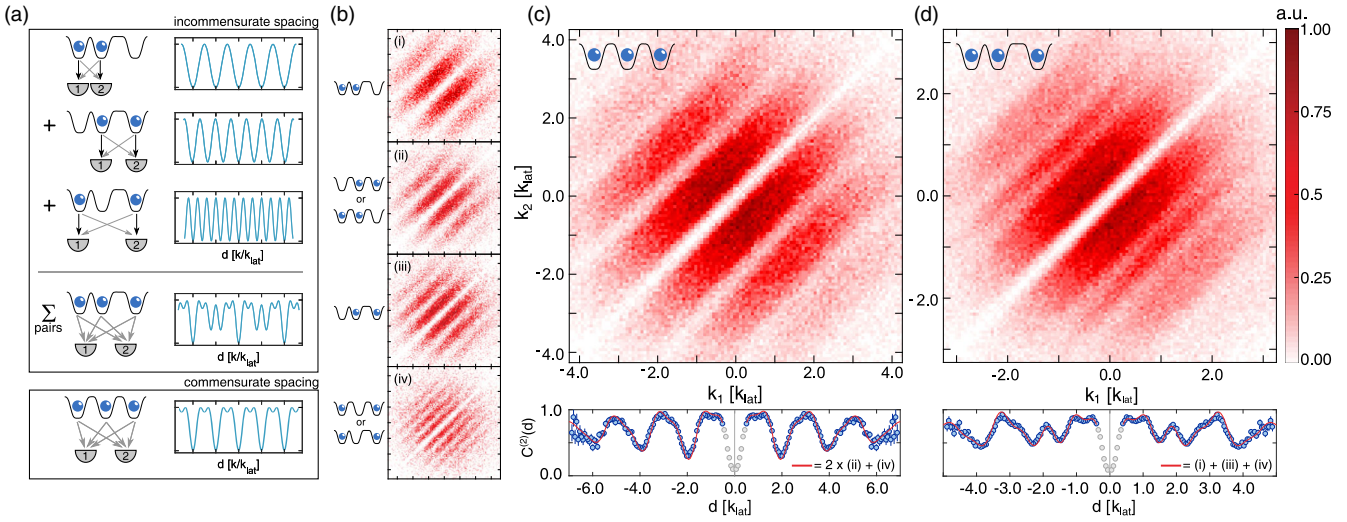

FIG. 3. Second-order correlations for three fermions. (a) Top: For an arbitrary configuration of single-fermion sources, each pair of particles contributes a sinusoidal oscillation to the correlation function $C^{(2)}(d)$. The full correlator can exhibit complex patterns due to beat notes between all spatial frequencies. Bottom: Expected full correlation function for three regularly spaced sources. (b) Correlators for individual pairs of sources. (c) Three particles released from three equidistant tweezers exhibit correlations at the momentum scale k_{lat} and its first harmonic, leading to a "superlattice" structure in $C^{(2)}(d)$. The bottom row displays the measured $C^{(2)}(d)$ for three particles (data points), together with a prediction (red line) given by the weighted sum of fits to the two-particle contributions from Fig. 3(b). (d) For three tweezers with irregular spacing, three distinct spatial frequencies contribute to the full second-order correlator. The sharp dip at $k_1 = k_2$ is partially due to our lack of sensitivity to coincidences at short distances.

be detected in our experiment [21]. We exclude these points from all further analysis. To quantify the strength of periodic correlations, we fit a damped cosine function to the correlations away from $d = 0$, which gives a modulation contrast of 79(2)%. The contrast certifies the high degree of indistinguishability between the particles during the preparation and the matter-wave expansion. With a ground state preparation fidelity of 97(2)%, one would in principle expect correlations with a contrast of up to ∼95%. The measured contrast is limited by alignment errors between the axis of the optical dipole trap and the axis connecting the tweezer, which provide some distinguishability between the particles during the expansion dynamics [21]. Nevertheless, the contrast significantly exceeds the minimum visibility of $1/\sqrt{2} \approx 71\%$ required to perform quantum optics experiments such as nonlocality tests with massive particles [28,29].

With this high-contrast on-demand source of indistinguishable fermions, we can now study second- and third-order correlations of a triplet of sources (Fig. 1). For a system of N localized sources each emitting a single fermionic particle, it can be shown that negative exchange symmetry gives rise to a second-order correlation function of the form

$$C^{(2)}(d) = \frac{2}{N^2} \sum_{\langle i,j \rangle}^{N} (1 - \cos(d(x_i - x_j))), \qquad (2)$$

where the summation runs over all distinct pairs of emitters, and x_i refers to the center of the ith source [21].

This expression gives an intuitive picture for the expected second-order momentum correlations [Fig. 3(a)]: Every pair of particles generates a sinusoidal antibunching signal with a spacing given by the inverse source separation. The full second-order correlation function is the sum over all pairwise correlation signals.

We probe the validity of this picture using three equidistant tweezers with $a_{12} = a_{23} = 2\ \mu$m, where a_{ij} refers to the spatial separation of tweezer i and j. Pairs from neighbouring tweezers contribute a "long wavelength" correlation signal at a scale of $k_{\mathrm{lat}} = \pi/a_{12} = \pi/a_{23}$, whereas the outermost tweezers 1 and 3 give rise to a "short wavelength" modulation with half the period of $\pi/a_{13} = k_{\mathrm{lat}}/2$. The two contributions should result in a superlattice correlation structure, shown in Fig. 3(a). Adding more sources, and hence Fourier components, would lead to narrower correlation minima and result in the delta-function correlations observed for fermionic band insulators [9].

Figure 3(b) shows the experimentally measured second-order correlations. We first record the correlator for every tweezer spacing individually by loading only two of the three microtraps. The pairwise correlations [shown in panels (i) to (iv) of Fig. 3(b)] are identical to the two-tweezer case in Fig. 2, with a correlation scale given by the inverse spacing of the active sources. Separately, we measure the full second-order correlator for all three tweezers loaded simultaneously [Fig. 3(c)].

The bottom panels of Figs. 3(c) and 3(d) show the correlation function $C^{(2)}(d)$ for the three-particle system

(blue data points). We test the applicability of Eq. (2) by a comparison to the two-tweezer contributions: We individually fit the correlation functions from Fig. 3(b) and show the weighted sum of the fits as the red line [21]. The three-particle second-order correlation function, including the decay of the contrast towards larger relative momenta d, is very well reproduced by the sum of the pair contributions.

For the above case of regularly spaced sources, all two-particle correlations occur at the lattice momentum scale and its first harmonic. Source arrays with irregular spacing, on the other hand, can result in distinct correlation signals from all pairs of emitters and complex structures in the full correlator [see Fig. 3(a)].

We study the case of three tweezers with nonequal spacing in Fig. 3(d), where $a_{12} = 1.6\ \mu$m and $a_{23} = 1.5a_{12} = 2.4\ \mu$m. The incommensurate spacing leads to a doubling of the unit cell to four times the momentum k_{lat}, which we define via the smallest tweezer spacing a_{12}. Also, here, the correlations in the three-particle system are in perfect agreement with the weighted contributions from pairs of sources.

To fully characterize the field produced by multiple sources, a measurement of correlation functions at higher orders is required. For bosonic particles, such measurements are routinely performed to assess the statistical properties of light sources [7,30,31]. Recently, measurements of higher-order correlations of massive bosonic particles have become possible with ultracold atoms [32–34].

We measure the statistical properties of the matter-wave field emanating from the three fermionic sources via the third-order correlator $\langle :\hat{n}_{k_1}\hat{n}_{k_2}\hat{n}_{k_3}: \rangle$ and the corresponding normalized correlation function

$$C^{(3)}(d_1, d_2) = \frac{\int \langle :\hat{n}_k \hat{n}_{k+d_1} \hat{n}_{k+d_2}: \rangle dk}{\int \langle \hat{n}_k \rangle \langle \hat{n}_{k+d_1} \rangle \langle \hat{n}_{k+d_2} \rangle dk}. \tag{3}$$

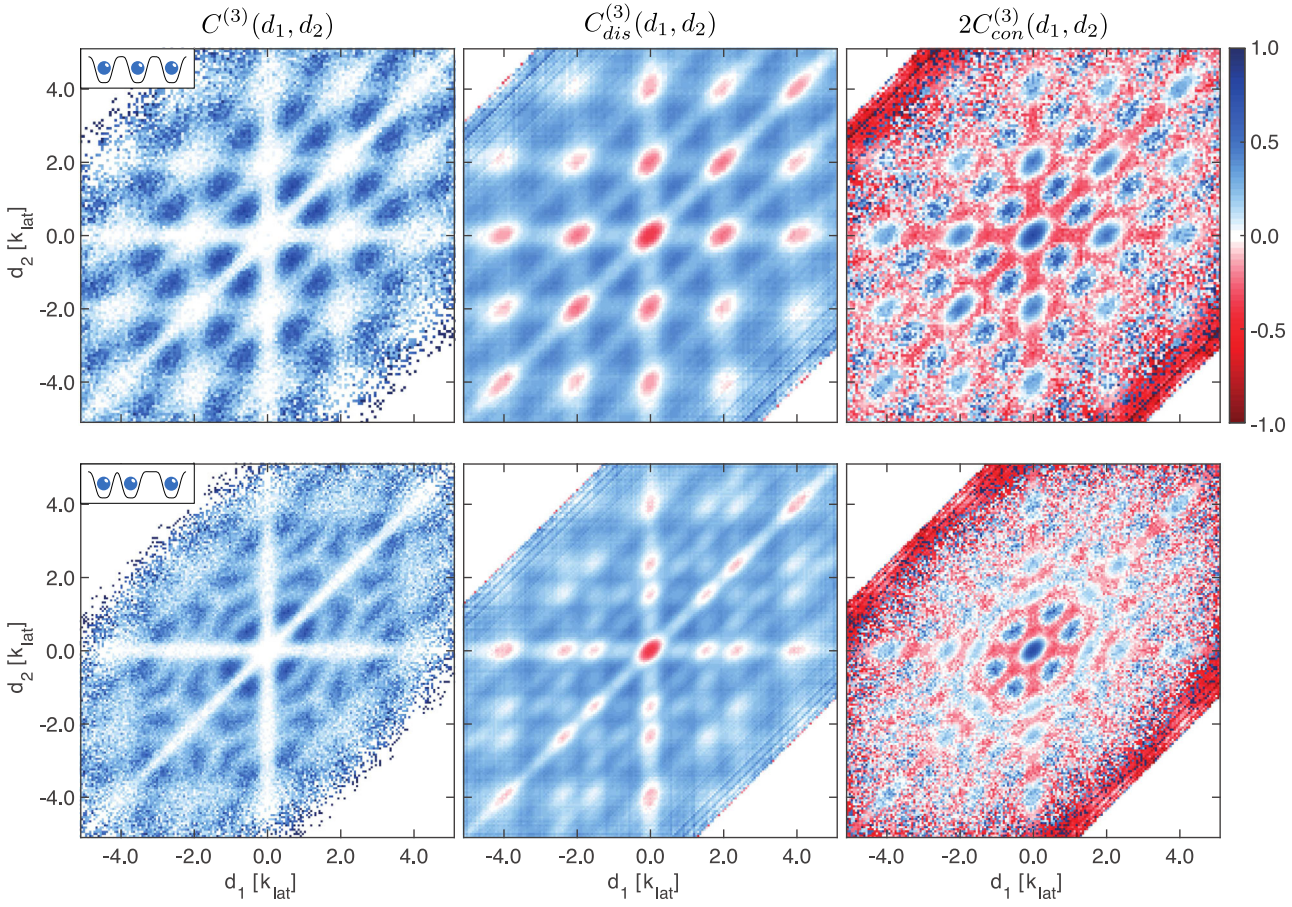

FIG. 4. Third-order momentum correlations. Normalized correlation function $C^{(3)}(d_1, d_2)$ for three fermions released from three wells with regular spacing ($a_{23} = a_{12}$, top row) and nonequal spacing ($a_{23} = 1.5a_{12}$, bottom row). The left column shows the full measured correlations, and the central and right columns show the disconnected and connected parts of the correlation function, respectively. By construction, the function is symmetric under the transformation $(d_1, d_2) \Leftrightarrow (-d_1, -d_2)$. The connected part of the correlation function $C^{(3)}_{\mathrm{con}}$ is scaled by a factor of two for better visibility. The measurement demonstrates the sensitivity to third-order correlations in the fermionic matter-wave field.

The correlation function is shown in Fig. 4 for the two datasets from Fig. 3. The equidistant and incommensurate tweezer configurations lead to clear and distinct correlation features at third order.

In order to interpret the third-order density correlations, it is useful to first remove contributions from lower order. This can be achieved by subtracting a suitable combination of first- and second-order correlators from the full third-order correlation function. Any remaining correlations are intrinsic; that is, they cannot be accessed from measurements at lower order. In interacting systems, such intrinsic correlations carry crucial information about the many-body state [33,34], but they may be present even for free particle systems [19,20]. For noninteracting bosons, e.g., the intrinsic correlations contribute to a striking increase in zero-distance correlations at higher order [30,32].

To assess the presence of intrinsic third-order correlations in our system, we combine our measurements at second order to construct the disconnected part of the third-order correlation function $C^{(3)}_{\mathrm{dis}}(d_1, d_2)$. We define the disconnected correlator as [19,20,33]

$$\begin{aligned}\langle :\hat{n}_{k_1}\hat{n}_{k_2}\hat{n}_{k_3}:\rangle_{\mathrm{dis}} = s_1(N)(&\langle \hat{n}_{k_1}\rangle\langle :\hat{n}_{k_2}\hat{n}_{k_3}:\rangle \\ &+ \langle \hat{n}_{k_2}\rangle\langle :\hat{n}_{k_1}\hat{n}_{k_3}:\rangle + \langle \hat{n}_{k_3}\rangle\langle :\hat{n}_{k_1}\hat{n}_{k_2}:\rangle) \\ &- 2s_2(N)\langle \hat{n}_{k_1}\rangle\langle \hat{n}_{k_2}\rangle\langle \hat{n}_{k_3}\rangle. \end{aligned} \quad (4)$$

The scale factors $s_1(N) = [N(N-1)(N-2)]/[N^2(N-1)]$ and $s_2(N) = [N(N-1)(N-2)]/N^3$ account for correlations due to particle number conservation [21] and approach unity as $N \to \infty$. The corresponding correlation function $C^{(3)}_{\mathrm{dis}}(d_1, d_2)$ represents the experimentally accessible knowledge of third-order correlations available from pairwise measurements and is shown in the central column of Fig. 4. Clearly, it does not include all features of the full correlation function, and the connected part of the correlation function, $C^{(3)}_{\mathrm{con}} = C^{(3)} - C^{(3)}_{\mathrm{dis}}$, retains additional structure, shown in the right-hand column of Fig. 4. The presence of intrinsic correlations agrees very well with an analytic calculation and is in full agreement with a decomposition according to Wick's theorem [21,35]. Recovering the expected functional form of third-order correlations for different spatial tweezer arrangements validates our analysis. We conclude that the system displays strong correlations at third order consistent with ideal fermionic statistics. To our knowledge, this constitutes the first experimental characterization of a fermionic field beyond second order and realizes the fermionic counterpart to the recent observation of three-photon interference [36,37].

Our work opens the door for several interesting avenues of research: Our high-purity on-demand source of indistinguishable fermions may enable quantum optics experiments with massive particles, such as fermionic ghost imaging or Bell tests [20,29,38]. Extending our methods to more particles and modes, the interplay of coherence, indistinguishability, and quantum statistics can be studied in many-fermion interference [1]. This is of particular interest in regards to the dynamics of many-body systems, which are given by a combination of interaction effects and the interference phenomena studied here [39].

We thank M. Gärttner, P. Hauke, C. Westbrook, and G. Zürn for insightful discussions. This work has been supported by ERC consolidator Grant No. 725636, DFG Grant No. JO970/1-1, the Heidelberg Center for Quantum Dynamics, and DFG Collaborative Research Centre Grant No. SFB 1225 (ISOQUANT). A. B. acknowledges funding from the International Max-Planck Research School (IMPRS-QD). P. M. P. acknowledges funding from the EU Horizon 2020 program under Marie Sklodowska-Curie Grant Agreement No. 706487 and the Daimler and Benz Foundation.

*preiss@physi.uni-heidelberg.de
†Present address: Institute for Quantum Electronics, ETH Zurich, 8093 Zurich, Switzerland.

[1] M. C. Tichy, Interference of identical particles from entanglement to boson-sampling, J. Phys. B **47**, 103001 (2014).
[2] R. Hanbury Brown and R. Q. Twiss, Correlation between photons in two coherent beams of light, Nature (London) **177**, 27 (1956).
[3] R. Hanbury Brown and R. Q. Twiss, A test of a new type of stellar interferometer on Sirius, Nature (London) **178**, 1046 (1956).
[4] R. Ghosh and L. Mandel, Observation of Nonclassical Effects in the Interference of Two Photons, Phys. Rev. Lett. **59**, 1903 (1987).
[5] C. K. Hong, Z. Y. Ou, and L. Mandel, Measurement of Subpicosecond Time Intervals between Two Photons by Interference, Phys. Rev. Lett. **59**, 2044 (1987).
[6] R. J. Glauber, The quantum theory of optical coherence, Phys. Rev. **130**, 2529 (1963).
[7] M. O. Scully and M. S. Zubairy, *Quantum Optics* (Cambridge University Press, Cambridge, England, U.K., 1997).
[8] G. Alexander, Bose-Einstein and Fermi-Dirac interferometry in particle physics, Rep. Prog. Phys. **66**, 481 (2003).
[9] T. Rom, T. Best, D. van Oosten, U. Schneider, S. Fölling, B. Paredes, and I. Bloch, Free fermion antibunching in a degenerate atomic Fermi gas released from an optical lattice, Nature (London) **444**, 733 (2006).
[10] M. Iannuzzi, A. Orecchini, F. Sacchetti, P. Facchi, and S. Pascazio, Direct Experimental Evidence of Free-Fermion Antibunching, Phys. Rev. Lett. **96**, 080402 (2006).
[11] T. Jeltes, J. M. McNamara, W. Hogervorst, W. Vassen, V. Krachmalnicoff, M. Schellekens, A. Perrin, H. Chang, D. Boiron, A. Aspect, and C. I. Westbrook, Comparison of the Hanbury Brown–Twiss effect for bosons and fermions, Nature (London) **445**, 402 (2007).
[12] H. Kiesel, A. Renz, and F. Hasselbach, Observation of Hanbury Brown–Twiss anticorrelations for free electrons, Nature (London) **418**, 392 (2002).

[13] W. D. Oliver, J. Kim, R. C. Liu, and Y. Yamamoto, Hanbury Brown and Twiss-type experiment with electrons, Science **284**, 299 (1999).
[14] M. Henny, S. Oberholzer, C. Strunk, T. Heinzel, K. Ensslin, M. Holland, and C. Schönenberger, The fermionic Hanbury Brown and Twiss experiment, Science **284**, 296 (1999).
[15] E. Bocquillon, V. Freulon, J.-M. Berroir, P. Degiovanni, B. Plaçais, A. Cavanna, Y. Jin, and G. Fève, Coherence and indistinguishability of single electrons emitted by independent sources, Science **339**, 1054 (2013).
[16] M. Waitz *et al.*, Two-Particle Interference of Electron Pairs on a Molecular Level, Phys. Rev. Lett. **117**, 083002 (2016).
[17] F. Serwane, G. Zürn, T. Lompe, T. B. Ottenstein, A. N. Wenz, and S. Jochim, Deterministic preparation of a tunable few-fermion system, Science **332**, 336 (2011).
[18] S. Murmann, A. Bergschneider, V. M. Klinkhamer, G. Zürn, T. Lompe, and S. Jochim, Two Fermions in a Double Well: Exploring a Fundamental Building Block of the Hubbard Model, Phys. Rev. Lett. **114**, 080402 (2015).
[19] C. D. Cantrell, *n*-fold photoelectric counting statistics of Gaussian light, Phys. Rev. A **1**, 672 (1970).
[20] H.-C. Liu, High-order correlation of chaotic bosons and fermions, Phys. Rev. A **94**, 023827 (2016).
[21] See Supplemental Material at http://link.aps.org/supplemental/10.1103/PhysRevLett.122.143602 for details on state preparation, data processing, and theoretical analysis.
[22] P. A. Murthy, D. Kedar, T. Lompe, M. Neidig, M. G. Ries, A. N. Wenz, G. Zürn, and S. Jochim, Matter-wave Fourier optics with a strongly interacting two-dimensional Fermi gas, Phys. Rev. A **90**, 043611 (2014).
[23] S. Fölling, F. Gerbier, A. Widera, O. Mandel, T. Gericke, and I. Bloch, Spatial quantum noise interferometry in expanding ultracold atom clouds, Nature (London) **434**, 481 (2005).
[24] A. Bergschneider, V. M. Klinkhamer, J. H. Becher, R. Klemt, G. Zürn, P. M. Preiss, and S. Jochim, Spin-resolved single-atom imaging of ^{6}Li in free space, Phys. Rev. A **97**, 063613 (2018).
[25] E. Altman, E. Demler, and M. D. Lukin, Probing many-body states of ultracold atoms via noise correlations, Phys. Rev. A **70**, 013603 (2004).
[26] I. B. Spielman, W. D. Phillips, and J. V. Porto, Mott-Insulator Transition in a Two-Dimensional Atomic Bose Gas, Phys. Rev. Lett. **98**, 080404 (2007).
[27] S. Fölling, *Quantum Gas Experiments: Exploring Many-Body States* (World Scientific, Singapore, 2015).
[28] P. Samuelsson, E. V. Sukhorukov, and M. Büttiker, Two-Particle Aharonov-Bohm Effect and Entanglement in the Electronic Hanbury Brown–Twiss Setup, Phys. Rev. Lett. **92**, 026805 (2004).
[29] M. Bonneau, W. J. Munro, K. Nemoto, and J. Schmiedmayer, Characterizing twin-particle entanglement in double-well potentials, Phys. Rev. A **98**, 033608 (2018).
[30] M. Aßmann, F. Veit, M. Bayer, M. van der Poel, and J. M. Hvam, Higher-order photon bunching in a semiconductor microcavity, Science **325**, 297 (2009).
[31] A. Singer, U. Lorenz, F. Sorgenfrei, N. Gerasimova, J. Gulden, O. M. Yefanov, R. P. Kurta, A. Shabalin, R. Dronyak, R. Treusch, V. Kocharyan, E. Weckert, W. Wurth, and I. A. Vartanyants, Hanbury Brown–Twiss Interferometry at a Free-Electron Laser, Phys. Rev. Lett. **111**, 034802 (2013).
[32] R. G. Dall, A. G. Manning, S. S. Hodgman, W. RuGway, K. V. Kheruntsyan, and A. G. Truscott, Ideal n-body correlations with massive particles, Nat. Phys. **9**, 341 (2013).
[33] T. Schweigler, V. Kasper, S. Erne, I. Mazets, B. Rauer, F. Cataldini, T. Langen, T. Gasenzer, J. Berges, and J. Schmiedmayer, Experimental characterization of a quantum many-body system via higher-order correlations, Nature (London) **545**, 323 (2017).
[34] S. S. Hodgman, R. I. Khakimov, R. J. Lewis-Swan, A. G. Truscott, and K. V. Kheruntsyan, Solving the Quantum Many-Body Problem via Correlations Measured with a Momentum Microscope, Phys. Rev. Lett. **118**, 240402 (2017).
[35] G. C. Wick, The evaluation of the collision matrix, Phys. Rev. **80**, 268 (1950).
[36] S. Agne, T. Kauten, J. Jin, E. Meyer-Scott, J. Z. Salvail, D. R. Hamel, K. J. Resch, G. Weihs, and T. Jennewein, Observation of Genuine Three-Photon Interference, Phys. Rev. Lett. **118**, 153602 (2017).
[37] A. J. Menssen, A. E. Jones, B. J. Metcalf, M. C. Tichy, S. Barz, W. S. Kolthammer, and I. A. Walmsley, Distinguishability and Many-Particle Interference, Phys. Rev. Lett. **118**, 153603 (2017).
[38] R. I. Khakimov, B. M. Henson, D. K. Shin, S. S. Hodgman, R. G. Dall, K. G. H. Baldwin, and A. G. Truscott, Ghost imaging with atoms, Nature (London) **540**, 100 (2016).
[39] T. Brünner, G. Dufour, A. Rodríguez, and A. Buchleitner, Signatures of Indistinguishability in Bosonic Many-Body Dynamics, Phys. Rev. Lett. **120**, 210401 (2018).